

Dehydrogenation of Indoline by Cytochrome P450 Enzymes: A Novel "Aromatase" Process

Hao Sun, William J. Ehlhardt, Palaniappan Kulanthaivel, Diane L. Lanza, Christopher A. Reilly, and Garold S. Yost

Department of Pharmacology and Toxicology, University of Utah, Salt Lake City, Utah (H.S., D.L.L., C.A.R. G.S.Y.); and Eli Lilly and Company, Lilly Corporate Center, Indianapolis, Indiana (W.J.E., P.K.)

Received February 19, 2007; accepted May 11, 2007

ABSTRACT

Indoline derivatives possess therapeutic potential within a variety of drug candidates. In this study, we found that indoline is aromatized by cytochrome P450 (P450) enzymes to produce indole through a novel dehydrogenation pathway. The indole products can potentially be bioactivated to toxic intermediates through an additional dehydrogenation step. For example, 3-substituted indoles like 3-methylindole and zafirlukast [4-(5-cyclopentyl-oxo-carbonylamino-1-methyl-indol-3-ylmethyl)-3-methoxy-*N*-*o*-tolylsulfonylbenzamide] are dehydrogenated to form 3-methyleneindolenine electrophiles, which react with protein and/or DNA nucleophilic residues to cause toxicities. Another potentially significant therapeutic consequence of indoline aromatization is that the product indoles might have dramatically different therapeutic potency than the parent indolines. In this study, indoline was indeed efficiently aromatized by human liver microsomes and by several P450s, but not by flavin-containing monooxygenase (FMO) 3. CYP3A4 had the

highest aromatase activity. Four additional indoline metabolites [2,3,4,7-tetrahydro-4,5-epoxy-1*H*-indole (M1); *N*-hydroxyindole (M2), *N*-hydroxyindoline (M3), and M4 ([1,4,2,5]dioxadiazino[2,3-*a*:5,6-*a'*]diindole)] were characterized; none was a metabolite of indole. M1 was an arene oxide from P450 oxidation, and M2, M3, and M4 were produced by FMO3. Our data indicated that indoline was oxidized to M3 and then to an intermediate indoline nitrene, which tautomerized to form M2, and subsequently dimerized to a di-indoline. This dimer was immediately oxidized by FMO3 or atmospheric oxygen to the final product, M4. No evidence was found for the P450-mediated production of an aliphatic alcohol from indoline that might dehydrate to produce indole. Therefore, P450 enzymes catalyze the novel "aromatase" metabolism of indoline to produce indole. The aromatase mechanism does not seem to occur through *N*-oxidation or dehydration of an alcohol but rather through a formal dehydrogenation pathway.

Indoline, 2,3-dihydroindole, is a "saturated" structural analog of indole. Indoline-containing drugs have been utilized as drug candidates in a variety of therapeutic fields and are more frequently employed in new therapeutic entities in recent years. Indolines have been widely investigated as serotonin receptor agonists or antagonists. Examples in-

clude: SB-242084, a selective 5-HT_{2C} receptor antagonist with anxiolytic activity (Bromidge et al., 1997); SB-224289, a selective 5-HT_{1B} receptor antagonist with negative intrinsic activity (Selkirk et al., 1998); and 1-(1-indolinyl)-2-propylamine, a 5-HT_{2C} receptor agonist for the treatment of obesity (Bentley et al., 2004). A series of potent factor Xa inhibitors, the indoline derivatives of DX-9065a, could be novel antithrombotics for the treatment and prevention of thromboembolic diseases (Noguchi et al., 2006). Another indoline derivative, 5-amino-1-(3,5-dimethylphenyl)-indoline, was reported as a selective cyclooxygenase-1 inhibitor for its antiangiogenic property (Sano et al., 2006). Other indoline

This study was supported by National Institutes of Health Grants GM074249 from the National Institutes of General Medical Sciences and HL013645 from the National Heart, Lung, and Blood Institute.

Article, publication date, and citation information can be found at <http://jpet.aspetjournals.org>.
doi:10.1124/jpet.107.121723.

ABBREVIATIONS: SB-242084, 6-chloro-5-methyl-1-[[2-[(2-methyl-3-pyridyl)oxy]-5-pyridyl]carbonyl]-indoline; SB-224289, 1'-methyl-5-[[2'-methyl-4'-(5-methyl-1,2,4-oxadiazol-3-yl)biphenyl-4-yl]carbonyl]-2,3,6,7-tetrahydro-spiro[furo[2,3-*f*]indole-3,4'-piperidine]; 5-HT, 5-hydroxytryptamine; DX-9065a, (+)-2*S*-2-[4-[[3*S*]-1-acetimidoyl-3-pyrrolidinyl]oxy]phenyl]-3-[7-amidino-2-naphthyl]propanoic acid; DW2282, (S)-(+)-4-phenyl-1-[1-(4-aminobenzoyl)-indoline-5-sulfonyl]-4,5-dihydro-2-imidazolone hydrochloride; zafirlukast, 4-(5-cyclopentyl-oxo-carbonylamino-1-methyl-indol-3-ylmethyl)-3-methoxy-*N*-*o*-tolylsulfonylbenzamide; P450, cytochrome P450; FMO, flavin-containing monooxygenase; GSH, glutathione; NAC, *N*-acetylcysteine; HPLC, high-performance liquid chromatography; LC/MS, liquid chromatography/mass spectrometry; M1, 2,3,4,7-tetrahydro-4,5-epoxy-1*H*-epoxy-1*H*-indole; M2, *N*-hydroxyindole; M3, *N*-hydroxyindoline; M4, [1,4,2,5]dioxadiazino[2,3-*a*:5,6-*a'*]diindole; ESI, electrospray ionization; APCI, atmospheric pressure chemical ionization; MS/MS, tandem mass spectrometry; CID, collision-induced dissociation; RO600175, 6-chloro-5-fluoro-1-(1-indolinyl)-2-propylamine.

derivatives that have been investigated recently include: DW2282, an anticancer agent (Hwang et al., 1999); 1-hexylindolinolactam-V, a protein kinase C-selective activator (Nakagawa et al., 2006); and indoline methotrexate, an antirheumatic agent (Matsuoka et al., 1996). A fascinating observation about indoline-containing therapeutic agents is that all of these drugs are under development, not commercially available yet. The lone exception is indapamide (Lozol), which is an indoline diuretic drug used to treat edema and hypertension (Sassard et al., 2005).

These indoline derivatives and the simple molecule indoline all share the same saturated pyrrole structure at the C-2 and C-3 position of the indoline ring and have at least one C-3 hydrogen atom available. 3-Substituted indoles, such as 3-methylindole, a pneumotoxicant, as well as zafirlukast, a leukotriene antagonist, are both dehydrogenated by cytochrome P450 enzymes to form 3-methyleneindolenine electrophiles. These electrophiles can subsequently react with protein and/or DNA nucleophilic residues to cause toxicities (Nocerini et al., 1984; Kassahun et al., 2005). The mechanism of P450-mediated dehydrogenation of 3-methylindole is believed to be initiated from 3-methyl hydrogen atom abstraction, followed by a second one-electron oxidation (Skiles and Yost, 1996). We speculated that proaromatic substrates like indoline and indoline derivatives mentioned above could be dehydrogenated by P450s, through an "aromatase" mechanism, to produce indoles, their aromatic products.

The dehydrogenation aromatase mechanism, reputedly occurring through two one-electron oxidation steps, is different from the CYP19-catalyzed aromatization, which contains a sequence of two-carbon oxidations and an oxidative carbon-carbon bond cleavage (Fishman, 1982). There are no studies to date that have described the aromatization of indolines by P450s, but the aromatization of 9,10-dihydrobenzo[e]pyrene, 1,2-dihydronaphthalene, 1,2-dihydroanthracene, 1,4-dihydropyridines, as well as *N*-alkyl-1,2,3,4-tetrahydroquinoline by rat liver microsomes and/or P450s was previously ob-

served (Wood et al., 1979; Guengerich and Bocker, 1988; Boyd et al., 1993; Gu et al., 2006). A dehydrogenation mechanism was proposed for the formation of naphthalene and anthracene from their dihydro compounds, rather than a mechanism of hydroxylation followed by dehydration (Boyd et al., 1993). From these observations and our previous dehydrogenation mechanism studies of 3-methylindole and zafirlukast, it was hypothesized that indoline may be dehydrogenated by P450s to form indole.

The purpose of the study presented here was to determine whether indole was formed by dehydrogenation of indoline by investigating the *in vitro* metabolism of indoline by human liver microsomes. To identify and structurally characterize some of the metabolites by mass spectrometry and ¹H NMR analysis, the metabolism of indoline by individual recombinant P450s and a readily available recombinant human flavin-containing monooxygenase (FMO) 3 was also conducted. The study utilized nucleophilic thiols, reduced glutathione (GSH), and *N*-acetylcysteine (NAC) to trap putative reactive intermediates that might be formed during indoline metabolism. In this study, in addition to describing the P450-mediated dehydrogenation aromatization pathway, the *N*-oxidation aromatization and dimerization/aromatization pathways catalyzed by FMO3 through indoline nitron formation and nitron cycloaddition were also characterized (Fig. 1).

Materials and Methods

Materials. Indoline, indole, oxindole, 4-hydroxyindole, NADPH, reduced GSH, NAC, and ammonium acetate were purchased from Sigma-Aldrich, Inc. (St. Louis, MO). 5-Bromoindoline, 5-bromo-7-nitroindoline, and 5-bromo-7-nitroindole were purchased from Lancaster Synthesis, Inc. (Pelham, NH). 5-Bromoindole and 6-nitroindole were purchased from Acros Organics USA (Morris Plains, NJ), and 6-nitroindoline was purchased from Alfa Aesar (Ward Hill, MA). Solvents used for HPLC, LC/MS, and NMR analysis were HPLC grade.

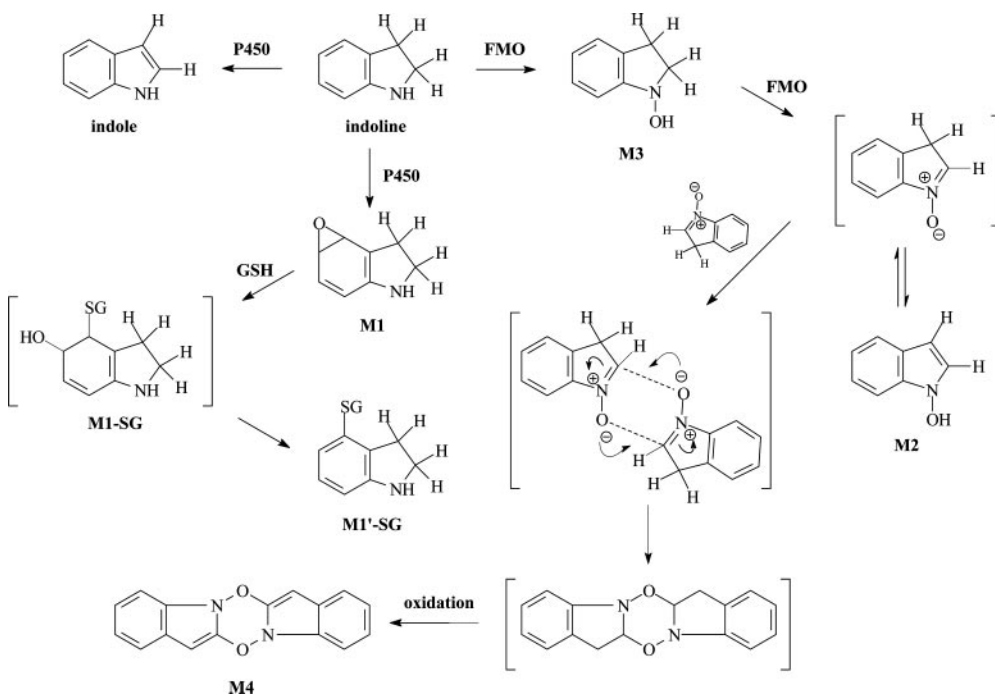


Fig. 1. Proposed indoline metabolism from P450 and FMO turnover. Brackets, putative intermediates. To simplify the figure, the structures of M1, M1'-SG, and M1-SG are shown as single regioisomers rather than the plethora of putative metabolites that could be produced by epoxidation and glutathione addition at other places on the aromatic ring. Mass spectral fragments of these metabolites did not permit us to assign specific regioisomer structures.

Incubations with Human Liver Microsomes. Pooled human liver microsomes (20 mg/ml protein) were obtained from BD Biosciences (San Jose, CA). Each incubation contained indoline (100 μ M), human liver microsomes (50 pmol of P450), NADPH (2 mM), and potassium phosphate buffer (0.1 M, pH 7.4) in a final volume of 75 μ l. The reaction was initiated by the addition of NADPH. The mixtures were incubated in a 37°C shaking water bath for various time points (5, 7.5, 10, 15, and 30 min) and were terminated by adding 75 μ l of ice-cold acetonitrile. After mixing with a vortex mixer and centrifugation at 21,000g for 30 min, the supernatant was collected and analyzed by HPLC and LC/MS. Incubations without NADPH were used as the negative controls. Indole (100 μ M) metabolism by human liver microsomes was also conducted under the same conditions.

Incubations with cDNA-Expressed Recombinant P450s. Individual cytochrome P450s that included CYP1A2, CYP2A6, CYP2B6, CYP2C8, CYP2C9, CYP2C19, CYP2D6, CYP2E1, and CYP3A4, containing both P450 reductase and cytochrome b_5 , were purchased from BD Biosciences. To compare the time course (5, 7.5, 10, 15, and 30 min) of the formation of the aromatization product indole by individual P450s (50 pmol), the same incubation and sample analysis conditions that were employed with human liver microsomes were used for each recombinant enzyme.

Incubations with FMO3. Human FMO3 supersomes were purchased from BD Biosciences. For determination of the time course of the production of metabolites M2 and M3 by FMO3, each incubation contained indoline (100 μ M), FMO3 (25 pmol), and NADPH (2 mM) and was incubated for various time points (0, 1, 2, 3, 5, 10, 15, 20, 30, 45, 60, or 120 min). The same sample work-up methods that were used for human liver microsomes were used for FMO3. The relative amounts of M2 and M3 production were measured by HPLC analysis. For samples used for structural characterization of M2, M3, and M4 by LC/MS analysis, the incubation time was 20 min, which was determined by time course analysis to be the optimal time point for both M2 and M3 formation.

Aromatization Kinetic Studies. To determine the aromatase kinetic parameters, for a series of incubations containing human liver microsomes or recombinant CYP1A2, CYP2B6, CYP2C19, CYP2D6, CYP2E1, or CYP3A4, the incubation time (10 min) and enzyme concentration (25 pmol), both within their linear range, were chosen for the substrate indoline (0–500 μ M), together with NADPH (2 mM) and 0.1 M potassium phosphate buffer, pH 7.4, in a final volume of 75 μ l. An equal volume of ice-cold acetonitrile was added to terminate the incubations. After centrifugation (30 min, 21,000g, at 4°C), 100 μ l of the supernatant was collected and immediately injected onto the HPLC column. The amount of indole formed at each substrate concentration was determined with a standard curve and used for kinetic analysis. Kinetic parameters including V_{\max} , the maximal velocity, and K_m , the substrate concentration at half-maximal velocity, were obtained by a nonlinear least-squares regression fitting of the Michaelis-Menten equation, $V = V_{\max} \times [S]/(K_m + [S])$, using the "Solver" function from Microsoft Excel 2002 (Microsoft, Redmond, WA).

HPLC Analysis of Indole Formation and Time Course of M2 and M3 Production. HPLC was performed on an Agilent 1100 system (Agilent Technologies, Inc., Palo Alto, CA) including an autosampler and a diode-array UV/VIS detector. The indoline metabolites from incubations with human liver microsomes, individual P450s, and FMO3 were separated using a Phenomenex Luna 5 μ C18 (250 \times 4.60 mm, 5 μ) reverse-phase column (Phenomenex Inc., Torrance, CA) at a flow rate of 1 ml/min. The mobile phase consisted of acetonitrile (solvent A) and 1 mM ammonium acetate (solvent B) with the gradient solvent program that was set as: 0 min, 10% A; 7 min, 35% A; 14 min, 50% A; 17 min, 55% A; 21 min, 95% A; 24 min, 95% A; and 32 min, 10% A. All samples were stored at 4°C in the autosampler before injection, unless otherwise specified. The separation was monitored with ultraviolet absorption at 270 nm for indole. A calibration curve of indole (peak area at 270 nm versus

concentration) was produced beforehand to quantify indole production in each sample. The relative amounts of M2 and M3 were determined as peak areas at multiple wavelengths (240, 270, and 280 nm).

Identification of Metabolites by LC/MS. All NADPH-dependent metabolites from incubations with human liver microsomes, individual P450s, as well as FMO3 were identified by LC/MS analysis using a Finnigan LCQ LC/MS system (Thermo Electron Corporation, Waltham, MA). Incubation samples were analyzed with a Phenomenex Luna 5 μ C18 (150 \times 2.00 mm, 5 μ) reverse-phase column (Phenomenex Inc.) with the mobile phase that consisted of acetonitrile (solvent A) and 1 mM ammonium acetate (solvent B) and eluted at a flow rate of 0.25 ml/min. The gradient system was set as: 0 min, 10% A; 7 min, 35% A; 14 min, 50% A; 17 min, 55% A; 22 min, 95% A; 32 min, 95% A; and 42 min, 10% A. The LC effluent was monitored with a UV-visible detector (Finnigan Surveyor PDA Detector; Thermo Electron Corporation) using a wavelength range from 200 to 700 nm before they were analyzed by the mass spectrometer (Finnigan LCQ Advantage MAX; Thermo Electron Corporation). Either an electrospray ionization (ESI) source or atmospheric pressure chemical ionization (APCI) source was used for the identification of metabolites by scanning the positive ions in the range of m/z 50 to 300. LC/ESI/MS was preferred for the ionization and detection of metabolites M1 and M3. The corresponding instrumental parameters were capillary temperature at 275°C, source voltage at 5000 V, capillary voltage at 26 V, and sheath gas flow rate at 50 units, which were determined to be the optimal condition for the standard indoline. LC/APCI/MS was the optimal method for the ionization and detection of metabolites M2 and indole. The instrumental parameters were then set as capillary temperature at 225°C, APCI vaporizer temperature at 350°C, source voltage at 6000 V, capillary voltage at 7 V, and sheath gas flow rate at 50 units, which were the optimal conditions for indole. Either LC/ESI/MS or LC/APCI/MS could be used for the ionization and detection of metabolite M4, and both were used for the MS/MS analysis of M4.

LC/MS/MS Identification of M4. LC/MS/MS was performed with either ESI/MS or APCI/MS using the same Finnigan LCQ system, C18 column (150 \times 2.00 mm), mobile phase and gradient system, as well as instrumental parameters as described above. M4 was identified by both LC/ESI/MS and LC/APCI/MS with m/z 263 (MH⁺); thus, the precursor ion at m/z 263 was selected for the collision-induced dissociation (CID) with the normalized collision energy at 35%, activation Q at 0.25, and activation time at 30 ms for ESI/MS or the normalized collision energy at 30%, activation Q at 0.25, and activation time at 30 ms for APCI/MS. The product ions at m/z 100 to 300 were scanned.

Identification of GSH Adduct of M1. Indoline was incubated with human liver microsomes and individual P450s as described above in the presence of GSH or NAC. The concentrations of GSH or NAC used in the experiments were 2 mM, the incubation time was 45 min, and the rest of the conditions were the same as described above for human liver microsomes in the absence of GSH or NAC. These samples were used to evaluate the relative changes in the amount of M1 in the presence of GSH or NAC and to measure amounts of the new product. Because of their efficiency in the production of M1, human liver microsomes, CYP2D6 and CYP3A4, were selected for a larger volume MS/MS sample preparation, which included indoline (100 μ M), enzyme (300 pmol), NADPH (2 mM), and GSH (2 mM) in a final volume of 450 μ l. After incubation at 37°C for 45 min, the reaction was terminated by the addition of 450 μ l of ice-cold acetonitrile, and then centrifuged at 21,000g for 30 min. The supernatant was collected and concentrated to approximately 50 μ l using a constant nitrogen gas flow at room temperature. The concentrated samples were then subjected to LC/MS/MS analysis using the same Finnigan LCQ system, C18 column (150 \times 2.00 mm) and mobile phase and gradient system as described above. The ESI source was used, and the instrumental parameters were: capillary temperature at 225°C, source voltage at 5000 V, capillary voltage at 21 V, and

sheath gas flow rate at 50 U. Both the molecular ion ($M+H^+$) at m/z 443 and the dehydrated fragment [$M-H_2O + H^+$] at m/z 425 were monitored, and the latter was selected for the CID, due to its higher abundance. The CID parameters were programmed as follows: the normalized collision energy at 26%, activation Q at 0.25, and activation time at 30 ms. The product ion spectra for MH^+ at m/z 425 were obtained, and the fragments were used to interpret the structure of the M1 glutathione conjugate.

1H NMR Analysis of M2. M2 was purified by HPLC using the HPLC analysis conditions described above, except the C18 column was a Phenomenex Luna 5μ C18 (250×2.00 mm, 5μ) reverse-phase column (Phenomenex Inc.). The incubations contained indoline (250 μ M), FMO3 (50 pmol), and NADPH (2 mM) in a final volume of 75 μ l of potassium phosphate buffer. After 60-min incubation at 37°C, the reaction was terminated and centrifuged as described above. Aliquots of 100 μ l of the supernatant were injected onto the column, and fractions containing M2 were manually collected. All collected samples were stored at -80° C. To prepare for NMR analysis, the accumulation of 10 collections (approximately 0.8 ml) was added to 2 volumes of D_2O . The mixture was then applied onto a preconditioned Waters HLB (30 mg) extraction cartridge (Waters Corporation, Milford, MA). The cartridge was preconditioned by first washing with 2 ml of methanol followed by 2 ml of D_2O . After applying M2, the cartridge was first washed with 3 ml of D_2O followed by 1 ml of CD_3CN in 0.2-ml aliquots. Each 0.2-ml aliquot was independently analyzed by NMR. The highest concentrations of M2 were detected in fractions 3 and 4 followed by 5. For the indoline, oxindole, and 4-hydroxyindole standards, 2 to 5 mg of each compound was dissolved in approximately 200 μ l of CD_3OD . The indole standard was dissolved in either CD_3OD or CD_3CN for NMR analysis.

NMR spectra were acquired either on an Inova 500-MHz system equipped with a 3-mm IFC indirect detection probe or on an Inova 600 MHz system equipped with a Cold probe (Varian Inc., Palo Alto, CA). Compounds were dissolved in either CD_3OD or CD_3CN as mentioned above, transferred to a 3-mm NMR tube, and sealed before analysis. Proton chemical shifts were referenced to the residual solvent signal at 3.3 ppm in CD_3OD and 1.93 ppm in CD_3CN . Two-dimensional NMR experiments, including DQFCOSY, HSQC, and HMBC, were performed using standard Varian pulse sequences.

Results

Metabolic Activation of Indoline by Human Liver Microsomes. Incubations of the substrate indoline with pooled human liver microsomes, individual P450 enzymes, and/or FMO3 produced five metabolites (indole, M1, M2, M3, and M4), all of which were observed to be produced in an NADPH-dependent manner. Indole and M1 formation were time-dependent and enzyme concentration-dependent. They were formed only by human liver microsomes and several P450s, but not by FMO3. M2, M3, and M4 were formed by FMO3 turnover of indoline but were not produced by any P450 enzyme. Table 1 summarizes the chromatographic and

TABLE 1
Chromatographic and spectral characterization of indoline and its major metabolites

Compound	t_R^a	MH^+	UV-Visible λ_{max}
	min		
Indoline	13.5	120.3	208, 238, 290
Indole	17.0	118.2	218, 270
M1	9.3	136.2	194, 266
M2	15.6	134.1	220, 272
M3	11.4	136.1	206, 238, 284
M4	14.8	263.2	228, 434

^a Retention time (t_R) was derived from experiments that were conducted under *Materials and Methods*.

spectral characteristics of these metabolites, using both UV-visible and LC/MS. Three metabolites (indole, M2, and M4) are aromatization products that are formed by either P450 or FMO3 enzymes from the proaromatic substrate indoline. Figure 1 illustrates putative mechanisms for the formation of these five metabolites, through three different metabolic pathways: 1) the dehydrogenation pathway to form indole, 2) the aromatic ring epoxidation pathway to form M1, and 3) the *N*-oxidation pathway to form M2, M3, and M4. None of them was a metabolite of indole, using the same in vitro incubation conditions that were used to generate them from indoline (data not shown).

Characterization of P450 Aromatase Activity. To characterize the scope of aromatase activity for individual P450 enzymes, CYP1A2, CYP2A6, CYP2B6, CYP2C8, CYP2C9, CYP2C19, CYP2D6, CYP2E1, and CYP3A4 were examined for their ability to produce indole. As shown in Fig. 2, CYP3A4 was the most efficient enzyme in the production of indole. The CYP1A2, CYP2B6, CYP2C19, CYP2D6, and CYP2E1 enzymes seemed to produce about the same relative amounts of indole, which were similar to the production by human liver microsomes. However, indoline dehydrogenation by the CYP2A6, CYP2C8, and CYP2C9 enzymes could not be detected (not included in Fig. 2). Kinetic constants were determined from triplicate incubations with analysis by Michaelis-Menten plots of indole formation by human liver microsomes and multiple recombinant P450 enzymes (Table 2). The enzyme efficiency (V_{max}/K_m) of CYP3A4 was the highest of all the enzymes. However, CYP2C19 had a much lower K_m (37 μ M) than any other enzyme.

The substrate acceptance for dehydrogenation of indolines by human liver microsomes and individual P450s was evaluated with three indoline derivatives: 5-bromoindoline, 6-nitroindoline, and 5-bromo-7-nitroindoline. Surprisingly, all three of the substituted indolines were oxidized to their respective indoles by human liver microsomes and several P450s with essentially identical kinetic constants (Table 2). Thus, even the highly electron withdrawing nitro group on the benzene ring did not reduce the electron density of sub-

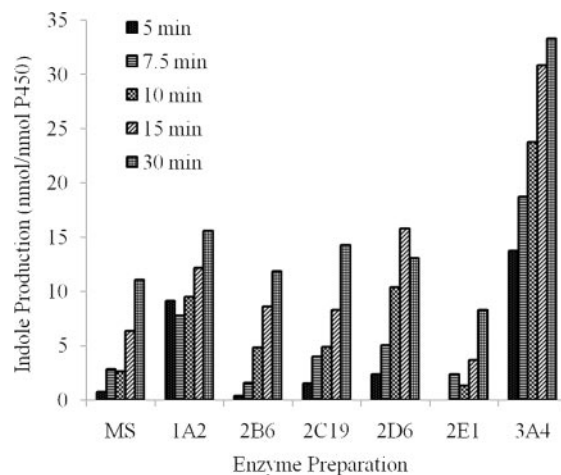


Fig. 2. Time dependence of indole production from indoline (100 μ M) in vitro by pooled human liver microsomes (50 pmol) or multiple recombinant cytochrome P450s (50 pmol). Incubations at 37°C included NADPH (2 mM) in potassium phosphate buffer (0.1 M, pH 7.4) in a final volume of 75 μ l. Production of indole was determined by LC/MS analysis as specified under *Materials and Methods*. All enzymes appeared to form indole in a linear manner.

TABLE 2

Kinetic constants for the formation of indoles by human liver microsomes and individual P450s

Compound	Enzyme	K_m μM	V_{max} min^{-1}	V_{max}/K_m $min^{-1} mM^{-1}$
Indoline	HLM	194	1.5	7.7
	CYP1A2	103	1.0	9.7
	CYP2B6	106	0.98	9.2
	CYP2C19	37	0.21	5.7
	CYP2D6	146	2.1	14.4
	CYP2E1	166	0.36	2.2
	CYP3A4	135	2.9	21.5
5-Bromoindoline	HLM	197	3.1	15.7
	CYP3A4	153	3.2	20.9
6-Nitroindoline	HLM	190	7.2	37.9
	CYP3A4	182	2.0	11.0
5-Br-7-nitroindoline	HLM	238	5.7	23.9
	CYP3A4	282	13.7	48.6

stituted indolines sufficiently to stop P450-mediated oxidation. Furthermore, no evidence with indoline or its analogs was found for the production of an aliphatic alcohol that might dehydrate to produce indole. Therefore, we concluded that several P450s serve as aromatases to catalyze indoline aromatization through dehydrogenation mechanisms, not through ring oxygenation and dehydration mechanisms.

GSH Adduct of M1. Metabolite M1 was a broad peak that eluted earlier than indoline and all other metabolites and disappeared upon addition of GSH or NAC to the incubations. Therefore, we opined that it was a reactive intermediate arene oxide that could be trapped by nucleophilic thiols. Analyses of the relative peak areas of M1 or its glutathione adduct after incubations of indoline with individual cDNA-expressed enzymes (CYP1A2, CYP2A6, CYP2B6, CYP2C8, CYP2C9, CYP2C19, CYP2D6, CYP2E1, and CYP3A4) indicated that CYP2D6 and CYP3A4 were the most efficient enzymes in the formation of M1, and CYP2D6 was slightly more efficient than CYP3A4.

LC/MS/MS was used to characterize the GSH adduct of M1. The molecular ion of the putative ring-opened epoxide at m/z 443 was detected but in very small amounts that could not be used to analyze daughter ions after collision-induced dissociation. Interestingly, the intensity of the ion at m/z 425 was 5- to 10-fold higher than the molecular ion. The m/z 425 ion (M1'-SG, Fig. 1) was probably produced by the loss of a water molecule after addition of GSH to the arene oxide (M1),

and this ion (labeled MH⁺ in Fig. 3) was used for MS/MS analysis. The LC/MS/MS product ion spectrum showed a characteristic loss of 129 atomic mass units at m/z 296 corresponding to the pyroglutamate residue of the GSH moiety (Baillie and Davis, 1993) and an additional loss of water at m/z 278. A plausible fragmentation pattern of the m/z 425 ion is presented in Fig. 3. This includes the loss of water to form an ion at m/z 407; the loss of CO₂ to form an ion at m/z 381; the cleavage of the α,β carbon-carbon bond of cysteine, combined with the loss of COOH at either the glycine or pyroglutamate moiety, to form product ions at m/z 215; as well as the double cleavage of C2 and C3 of the indoline ring and an additional loss of CO to produce an ion at m/z 369, from which an additional loss of glycine produced an ion at m/z 295.

FMO3-Catalyzed Indoline Aromatization. The time course of formation of metabolites M2 and M3 by FMO3 is shown in Fig. 4. The relative maximal amount of M3 was attained at approximately 20 min, which then decreased until this metabolite could not be detected in the incubation mixture at 2 h. However, the relative amounts of M2 increased steadily and appeared to attain maximal levels after approximately 2 h. The production and subsequent disappearance of M3 from incubations of indoline with FMO3 implied that it was formed but then metabolized by this enzyme.

Spectral (UV-visible) analysis of M2 showed that it was very similar to indole and that M3 was very similar to indo-

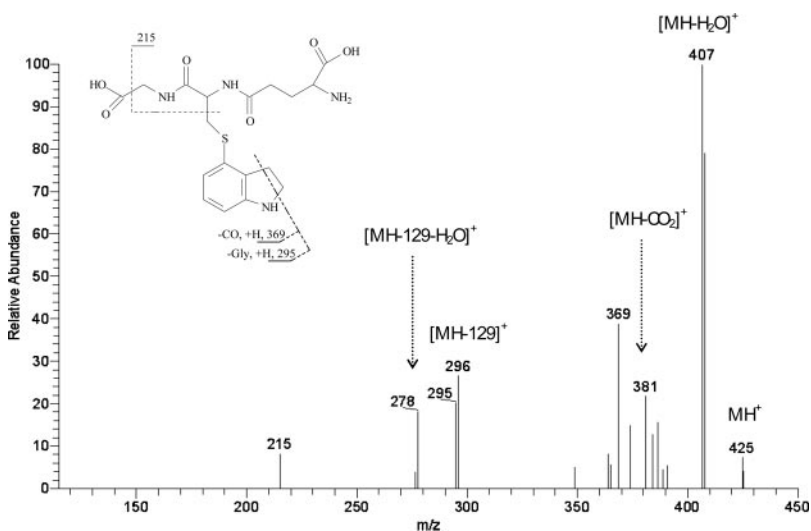


Fig. 3. LC/MS/MS product ion spectrum obtained by collision-induced dissociation of the $M+H^+$ ion (m/z 425) of the glutathione conjugate (M1'-SG) of the epoxide, M1. M1'-SG was presumably formed by dehydration of M1-SG in the mass spectrometer. The putative assignments of characteristic fragment ions are shown.

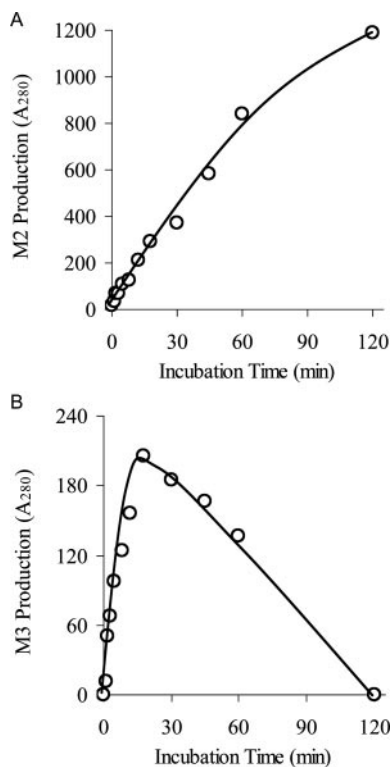


Fig. 4. Time course of metabolites M2 (A) and M3 (B) formation in incubations with the recombinant human FMO3 enzyme.

line (Table 1). The molecular ions of M2 and M3 were determined by LC/MS to be 134 and 136, respectively, which were consistent with the addition of oxygen to indoline to form *N*-hydroxyindoline (M3) and the aromatization of indoline and addition of oxygen to form *N*-hydroxyindole (M2). Other structures that placed the oxygen anywhere on the aromatic ring would not be consistent with the UV-visible spectra because the wavelength of the maximal absorption would have undergone a bathochromic shift. However, the UV-visible spectra of M2 closely mimicked an unsubstituted indole, and M3 closely mimicked an unsubstituted indoline.

Proton NMR was used to exclude structures where the oxygen was placed on C-2 or C-3 of indoline to form alcohols (m/z 136) or where oxygen was placed on C-2 of indole (oxindole, m/z 134) or on C-3 of indole (m/z 134). M2 accounted for approximately 90% of the metabolites of indoline that were formed by FMO3. The efficient production of M2 facilitated collection of larger quantities of this metabolite from the HPLC eluate for NMR analysis. The ¹H NMR of M2 was compared with several authentic indole standards to determine, partially by an elimination process, where the oxygen

TABLE 3

¹H NMR chemical shift assignments for M2 compared with several indole standards

Compound	Chemical Shifts ^a (ppm), Multiplicity (<i>J</i> in Hz)					
	H2	H3	H4	H5	H6	H7
Indoline ^b	3.42t (8.5)	2.96t (8.5)	7.07d (7.5)	6.67t (7.5)	6.95t (7.5)	6.66d (7.5)
Indole ^c	7.24d (2.8)	6.46d (2.8)	7.57d (8.0)	7.03t (8.0)	7.12t (8.0)	7.43d (8.0)
Oxindole ^b		3.48s	7.21d (7.5)	6.97t (7.5)	7.17t (7.5)	6.86d (7.5)
4-Hydroxyindole ^b	7.07d (3.2)	6.51d (3.2)		6.38m	6.89m	6.89m
M2 ^c	7.28d (3.0)	6.33d (3.0)	7.55d (8.0)	7.05t (8.0)	7.20t (8.0)	7.41d (8.0)

^a s, singlet; d, doublet; t, triplet; m, multiplet.

^b Recorded in CD₃OD.

^c Recorded in CD₃CN.

should be placed. These results (Table 3) showed that the chemical shifts and coupling constants of M2 were essentially identical to indole but much different from the other standards such as indoline, oxindole, or 4-hydroxyindole. Thus, we believe that M2 is *N*-hydroxyindole.

The structural assignments permitted us to postulate a metabolic scheme (Fig. 1). In this pathway, we postulate that the substrate indoline was *N*-oxidized by FMO3 to *N*-hydroxyindoline (M3) and then oxidized again to form indoline nitron, which tautomerized to produce the thermodynamically more stable *N*-hydroxyindole (M2). The metabolite M3 was formed in incubations of indoline with FMO3, but, interestingly, it was not detectable in incubations with human liver microsomes or in incubations that included both recombinant FMO3 and recombinant CYP3A4. These results indicate that M3 was formed by FMO3 and subsequently was a substrate for P450 oxidation. M2 was efficiently produced in these incubations, so it seems reasonable to propose that M2 was formed by P450 dehydrogenation of M3, through a process similar to the aromatase mechanism of P450-mediated dehydrogenation of indoline to indole.

Metabolite M4 was characterized by LC/MS/MS and UV-visible as a dimer that was possibly formed from indoline nitron (Fig. 1; Table 1). The MS/MS fragmentation (Fig. 5) showed that the structure of the M4 molecule was consistent with a 1,3-dipolar cycloaddition of indoline nitron, followed by oxidation (either FMO3-mediated or molecular oxygen-mediated) to finally produce the stable dimer, M4. M4 is a novel blue pigment that is different from indirubin and indigo, both of which are metabolites of indole (Gillam et al., 2000). All three pigments share the same molecular ions at m/z 263, but indigo and indirubin eluted at 20 and 18.5 min, respectively, which was later than indole (17 min), and M4 eluted earlier (at 14.8 min) than indole (Table 1). Furthermore, the characteristic visible spectra of indirubin and indigo have maximal absorption wavelengths at 552 and 603 nm, respectively (Gillam et al., 2000), but M4 had a λ_{\max} at 434 nm (Fig. 5). We believe that M4 is a novel indole pigment that is formed by FMO3 turnover of indoline. To our knowledge, this pigment has not been previously identified. In our experiments, we did not observe the "di-indoline" precursor of M4, probably because it was very quickly oxidized to M4, either by molecular oxygen or FMO3. In fact, M2 was slowly (several days) but completely converted to M4, while it was dissolved in CD₃OD at room temperature in an NMR tube (data not shown). Therefore, dimerization of indoline nitron and oxidation of the di-indoline by molecular oxygen appear to be thermodynamically favored chemical transformations.

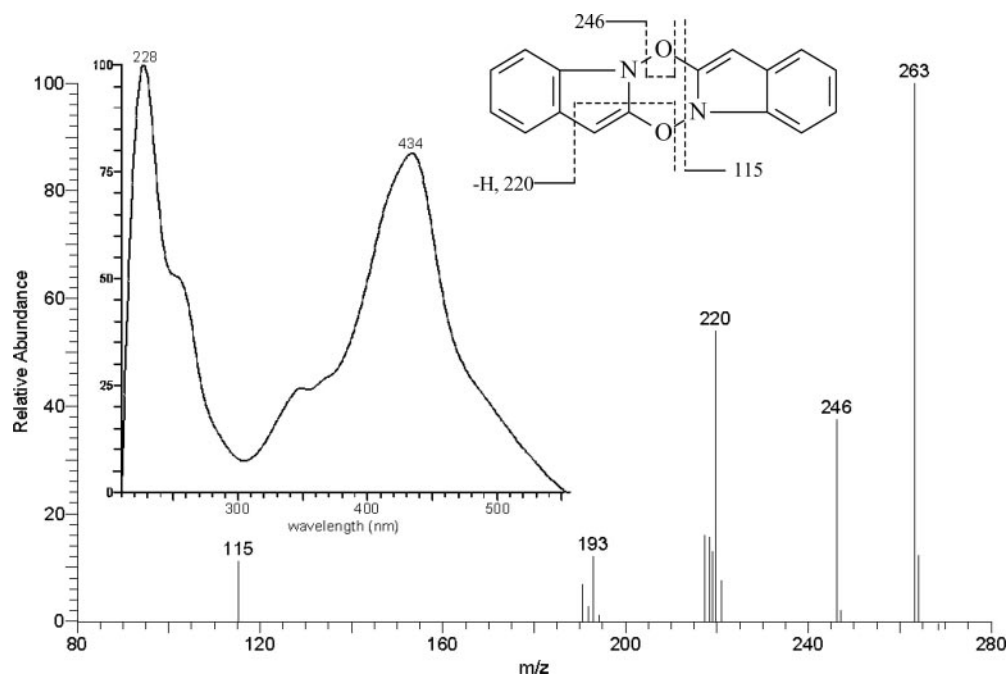


Fig. 5. Representative LC/MS/MS spectrum of the dimeric indoline metabolite M4, produced from incubations with human FMO3. The putative assignments of characteristic fragment ions are shown. Inset, UV-visible absorbance spectrum of M4.

Discussion

The results presented here show that the novel dehydrogenation metabolite indole was formed from indoline by human liver microsomes and several cytochrome P450 enzymes. In addition, we also identified a P450-catalyzed epoxide metabolite of indoline as well as several *N*-oxidation products that were formed by FMO3 catalysis. We have previously shown that multiple substrates, such as 3-methylindole, zafirlukast, and capsaicin (Reilly and Yost, 2005), are dehydrogenated by various P450 enzymes and have now extended our studies on dehydrogenation to evaluate proaromatic substrates like indoline. The results from the current study demonstrate that the proaromatic substrate indoline is indeed a suitable substrate for dehydrogenation and is aromatized to form indole. In fact, we have recently examined seven indoline-containing compounds and found that all were dehydrogenated by human liver microsomes and recombinant CYP3A4 (H. Sun and G. S. Yost, unpublished data).

A potential consequence of the aromatization reaction of therapeutic agents is that the indole metabolites might have significantly different pharmacological activities than the original compound. The indole derivative of factor Xa showed dramatic change in the inhibition activity in comparison to its corresponding indoline analog (Noguchi et al., 2006). It was demonstrated that the inhibitory activity was decreased over 300-fold by replacing the indoline ring ($IC_{50} = 11$ nM) with an indole ring ($IC_{50} = 3600$ nM). Others (Nakagawa et al., 2006) have reported that the indoline form of indolactam-V bound to kinase C much better than its indole form. These examples confirm our hypothesis that P450-mediated dehydrogenation of indolines can robustly decrease the potency of therapeutic agents.

Conversely, in another study (Bromidge et al., 1997) with a series of 5-HT_{2C} receptor agonists, RO600175 was a very potent 5-HT_{2C} receptor agonist, but its corresponding indoline analog showed significantly lower binding affinity (6-fold less). Therefore, aromatization of indoline-containing thera-

peutic agents by P450-mediated dehydrogenation can potentially alter the biological activity in either direction; therefore, the relative effects cannot be predicted de novo in patients. We found approximately 50% 5-bromo-7-nitro-indoline was aromatized to its indole form by human liver microsomes in a 30-min incubation (kinetics shown in Table 2); therefore, this route could potentially be the major metabolic route of drugs containing the indoline moiety. However, it should be noted that the K_m values of several P450 enzymes for indoline and several substituted indolines exceed 100 μ M, which might be too high for efficient enzyme turnover under normal physiological conditions.

To our knowledge, there are no examples of endogenous indoline-containing compounds that would serve as substrates for this aromatase reaction. Interestingly, we found that a significant majority of indoline-containing therapeutic agents are new entities, not drugs that are currently available. Therefore, it appears that pharmaceutical companies are utilizing the indoline structure more frequently in current drug development efforts than in the past. We would suggest that this novel cytochrome P450 aromatase activity should be carefully monitored when the metabolism of a new indoline-containing drug is evaluated.

Another metabolic pathway that is normally considered to cause toxicity is the epoxidation reaction (Lau and Zannoni, 1979; Guengerich, 2003). In our previous studies of 3-methylindole oxidation by P450s, in addition to characterization of the dehydrogenation pathway, we found evidence that supported the formation of 2,3-epoxy-3-methylindole, a reactive electrophile that could alkylate protein and nucleic acids (Skordos et al., 1998). In addition, we have recently published new studies that confirm the presence of at least two epoxides on the benzene ring of 3-methylindole (Yan et al., 2007). In the current results, we characterized M1, an arene oxide of indoline, through direct LC/MS results, and through the characterization of its GSH adduct. It was confirmed that M1 was not a 2,3-epoxide of indole by the interpretation of its

MS/MS fragmentation. Theoretically, GSH could conjugate at different positions such as C-5 or C-6 of the indoline aromatic ring, but the mass spectral fragmentation pattern did not permit us to establish the location of the GSH adduct. NMR could be used for this purpose, but the amounts of the GSH adduct were too small to collect enough adduct for this purpose.

Metabolism of indoline by FMO3 produced three more metabolites. Pig liver FMO *N*-oxidized desmethylpromethazine to a secondary hydroxylamine that additionally formed a nitron (Clement et al., 1993). A similar metabolic pathway was proposed for the oxidation of *N*-hydroxynorzimeldine (Cashman et al., 1990). In those studies, the nitron intermediate decomposed to a primary hydroxylamine and an aldehyde. Others (Rodriguez et al., 1999; Cerny and Hanzlik, 2005) have also reported the same hydroxylamine to nitron pathway of FMO-catalyzed oxidation of *N*-benzyl-*N*-cyclopropylamine and *N*-deacetylketonazole. The nitron intermediates from both compounds decomposed to the primary hydroxylamines and the aldehydes. Our studies of the FMO3-catalyzed oxidation of indoline also showed a sequential *N*-oxidation pathway (i.e., the sequential formation of M3, a hydroxylamine, to M2, the tautomerized nitron). However, instead of the nitron decomposing to a hydroxylamine and an aldehyde as the final products, oxidation of *N*-hydroxyindoline led to the nitron that tautomerized to *N*-hydroxyindole, a more stable aromatized structure.

Incubations of indoline with only FMO3 (without presence of P450 enzymes) also produced an oxidized dimer of indoline nitron, [1,4,2,5]dioxadiazino[2,3-*α*:5,6-*a'*]diindole. This metabolite (M4) was identified and characterized in this study. A typical reaction of nitron is the cycloaddition to other 1,3-diploes (either homo- or hetero-) (Hamer and Macaluso, 1964; Breuer, 1989). It has been known that a six-membered cyclic nitron, 3,4,5,6-tetrahydropyridine *N*-oxide, could be dimerized by this cycloaddition mechanism as a result of dipole-dipole interaction (Hamer and Macaluso, 1964; Breuer, 1989). This symmetrical dimer formed quickly without the help of any catalyst. We postulate that the indoline nitron metabolite could form a dimeric precursor to M4, 6*a*,7,13*a*,14-tetrahydro-[1,4,2,5]dioxadiazino[2,3-*α*:5,6-*a'*]diindole, which subsequently forms M4 by an additional oxidation reaction. The extended conjugation of the aromatic ring system of M4 is consistent with its visible absorbance spectrum. Unlike indigo or indirubin, which were formed through oxidized indoxyl and isatin in the oxidation of indole by P450 enzymes (Gillam et al., 2000), the formation of M4 proceeds through an indoline nitron pathway in the oxidation of indoline by FMO3. The M4 metabolite that was characterized in the current work would introduce a new pigment that was produced by FMO3 oxidation of indoline and may have potential applications, such as a new method in commercial dye production.

In conclusion, in these studies, we have demonstrated that indoline can be aromatized by several P450s to form indole through a dehydrogenation mechanism. A P450-catalyzed arene oxide metabolite was also partially characterized through its mass spectrum and the identification of its corresponding GSH adduct. We also found that FMO3 catalyzed the *N*-oxidation of indoline through indoline nitron to form two aromatized final products, *N*-hydroxyindole and [1,4,2,5]dioxadiazino[2,3-*α*:5,6-*a'*]diindole. Future studies

should clarify the dehydrogenation aromatase mechanism by selective P450 enzymes, through the investigation of the structural and conformational characteristics of a series of indoline derivatives, as well as the spatial and electronic parameters of active sites of these enzymes. In particular, it will be important to determine whether dehydrogenation proceeds through initial C-H bond hydrogen atom abstraction from the C-2 or C-3 positions or by nitrogen one-electron oxidation mechanisms.

References

- Baillie TA and Davis MR (1993) Mass spectrometry in the analysis of glutathione conjugates. *Biol Mass Spectrom* **22**:319–325.
- Bentley JM, Adams DR, Bebbington D, Benwell KR, Bickerdike MJ, Davidson JE, Dawson CE, Dourish CT, Duncton MA, Gaur S, et al. (2004) Indoline derivatives as 5-HT(2C) receptor agonists. *Bioorg Med Chem Lett* **14**:2367–2370.
- Boyd DR, Sharma ND, Agarwal R, McMordie RA, Bessems JG, van Ommen B, and van Bladeren PJ (1993) Biotransformation of 1,2-dihydronaphthalene and 1,2-dihydroanthracene by rat liver microsomes and purified cytochromes P-450: formation of arene hydrates of naphthalene and anthracene. *Chem Res Toxicol* **6**:808–812.
- Breuer E (1989) Nitrones and nitronic acid derivatives: their structure and their roles in synthesis, in *Nitrones, Nitronates and Nitroxides* (Patai S and Rappoport Z eds) pp 139–244, John Wiley & Sons Ltd., Chichester, UK.
- Bromidge SM, Duckworth M, Forbes IT, Ham P, King FD, Thewlis KM, Blaney FE, Naylor CB, Blackburn TP, Kennett GA, et al. (1997) 6-Chloro-5-methyl-1-[[2-(2-methyl-3-pyridyl)oxy]-5-pyridyl]carbonyl]-indoline (SB-242084): the first selective and brain penetrant 5-HT_{2C} receptor antagonist. *J Med Chem* **40**:3494–3496.
- Cashman JR, Yang ZC, and Hogberg T (1990) Oxidation of *N*-hydroxynorzimeldine to a stable nitron by hepatic monooxygenases. *Chem Res Toxicol* **3**:428–432.
- Cerny MA and Hanzlik RP (2005) Cyclopropylamine inactivation of cytochromes P450: role of metabolic intermediate complexes. *Arch Biochem Biophys* **436**:265–275.
- Clement B, Lustig KL, and Ziegler DM (1993) Oxidation of desmethylpromethazine catalyzed by pig liver flavin-containing monooxygenase: number and nature of metabolites. *Drug Metab Dispos* **21**:24–29.
- Fishman J (1982) Biochemical mechanism of aromatization. *Cancer Res* **42**:3277s–3280s.
- Gillam EM, Notley LM, Cai H, De Voss JJ, and Guengerich FP (2000) Oxidation of indole by cytochrome P450 enzymes. *Biochemistry* **39**:13817–13824.
- Gu C, Collins R, Holsworth DD, Walker GS, and Voorman RL (2006) Metabolic aromatization of *N*-alkyl-1,2,3,4-tetrahydroquinoline substructures to quinolinium by human liver microsomes and horseradish peroxidase. *Drug Metab Dispos* **34**:2044–2055.
- Guengerich FP (2003) Cytochrome P450 oxidations in the generation of reactive electrophiles: epoxidation and related reactions. *Arch Biochem Biophys* **409**:59–71.
- Guengerich FP and Bocker RH (1988) Cytochrome P-450-catalyzed dehydrogenation of 1,4-dihydropyridines. *J Biol Chem* **263**:8168–8175.
- Hamer J and Macaluso A (1964) Nitrones. *Chem Rev* **64**:473–495.
- Hwang HS, Moon EY, Seong SK, Choi CH, Chung YH, Jung SH, Lee DK, and Yoon SJ (1999) Characterization of the anticancer activity of DW2282, a new anticancer agent. *Anticancer Res* **19**:5087–5093.
- Kassahun K, Skordos K, McIntosh I, Slaughter D, Doss GA, Baillie TA, and Yost GS (2005) Zafirlukast metabolism by cytochrome P450 3A4 produces an electrophilic alpha, beta-unsaturated iminium species that results in the selective mechanism-based inactivation of the enzyme. *Chem Res Toxicol* **18**:1427–1437.
- Lau SS and Zannoni VG (1979) Hepatic microsomal epoxidation of bromobenzene to phenols and its toxicological implication. *Toxicol Appl Pharmacol* **50**:309–318.
- Matsuoka H, Kato N, Tsuji K, Maruyama N, Suzuki H, Mihara M, Takeda Y, and Yano K (1996) Antirheumatic agents. I. Novel methotrexate derivatives bearing an indoline moiety. *Chem Pharm Bull* **44**:1332–1337.
- Nakagawa Y, Irie K, Yanagita RC, Ohigashi H, Tsuda K, Kashiwagi K, and Saito N (2006) Design and synthesis of 8-octyl-benzolactam-V9, a selective activator for protein kinase C epsilon and eta. *J Med Chem* **49**:2681–2688.
- Nocerini MR, Carlson JR, and Yost GS (1984) Electrophilic metabolites of 3-methylindole as toxic intermediates in pulmonary oedema. *Xenobiotica* **14**:561–564.
- Noguchi T, Tanaka N, Nishimata T, Goto R, Hayakawa M, Sugidachi A, Ogawa T, Asai F, Matsui Y, and Fujimoto K (2006) Indoline derivatives I: synthesis and factor Xa (FXa) inhibitory activities. *Chem Pharm Bull* **54**:163–174.
- Reilly CA and Yost GS (2005) Structural and enzymatic parameters that determine alkyl dehydrogenation/hydroxylation of capsaicinoids by cytochrome P450 enzymes. *Drug Metab Dispos* **33**:530–536.
- Rodriguez RJ, Proteau PJ, Marquez BL, Hetherington CL, Buckholz CJ, and O'Connell KL (1999) Flavin-containing monooxygenase-mediated metabolism of *N*-deacetyl ketoconazole by rat hepatic microsomes. *Drug Metab Dispos* **27**:880–886.
- Sano H, Noguchi T, Miyajima A, Hashimoto Y, and Miyachi H (2006) Anti-angiogenic activity of basic-type, selective cyclooxygenase (COX)-1 inhibitors. *Bioorg Med Chem Lett* **16**:3068–3072.
- Sassard J, Bataillard A, and McIntyre H (2005) An overview of the pharmacology and clinical efficacy of indapamide sustained release. *Fundam Clin Pharmacol* **19**:637–645.
- Selkirk JV, Scott C, Ho M, Burton MJ, Watson J, Gaster LM, Collin L, Jones BJ,

- Middlemiss DN, and Price GW (1998) SB-224289: a novel selective (human) 5-HT_{1B} receptor antagonist with negative intrinsic activity. *Br J Pharmacol* **125**:202–208.
- Skiles GL and Yost GS (1996) Mechanistic studies on the cytochrome P450-catalyzed dehydrogenation of 3-methylindole. *Chem Res Toxicol* **9**:291–297.
- Skordos KW, Skiles GL, Laycock JD, Lanza DL, and Yost GS (1998) Evidence supporting the formation of 2,3-epoxy-3-methylindoline: a reactive intermediate of the pneumotoxin 3-methylindole. *Chem Res Toxicol* **11**:741–749.
- Wood AW, Levin W, Thakker DR, Yagi H, Chang RL, Ryan DE, Thomas PE, Dansette PM, Whittaker N, Turujman S, et al. (1979) Biological activity of benzo[a]pyrene: an assessment based on mutagenic activities and metabolic profiles of the polycyclic hydrocarbon and its derivatives. *J Biol Chem* **254**:4408–4415.
- Yan Z, Easterwood LM, Maher N, Torres R, Huebert N, and Yost GS (2007) Metabolism and bioactivation of 3-methylindole by human liver microsomes. *Chem Res Toxicol* **20**:140–148.

Address correspondence to: Dr. Garold S. Yost, Department of Pharmacology and Toxicology, University of Utah, 30 South 2000 East, Room 201, Salt Lake City, UT 84112-5820. E-mail: gyost@pharm.utah.edu
